

Short Intense Laser Pulse Collapse in Near-Critical Plasma

F. Sylla, A. Flacco, S. Kahaly, M. Veltcheva, A. Lifschitz, and V. Malka
*Laboratoire d'Optique Appliquée, ENSTA, CNRS,
Ecole Polytechnique, UMR 7639, 91761 Palaiseau, France*

E. d'Humières and V. Tikhonchuk

University Bordeaux - CNRS - CEA, Centre Lasers Intenses et Applications, UMR 5107, 33405 Talence, France

(Dated: November 4, 2018)

It is observed that the interaction of an intense ultra-short laser pulse with an overdense gas jet results in the pulse collapse and the deposition of a significant part of energy in a small and well localized volume in the rising part of the gas jet, where the electrons are efficiently accelerated and heated. A collisionless plasma expansion over $\sim 150 \mu\text{m}$ at a sub-relativistic velocity ($\sim c/3$) has been optically monitored in time and space, and attributed to the quasistatic field ionization of the gas associated to the hot electron current. Numerical simulations in good agreement with the observations suggest the acceleration in the collapse region of relativistic electrons, along with the excitation of a sizeable magnetic dipole that sustains the electron current over several picoseconds. Perspectives of ion beam generation at high repetition rate directly from gas jets are discussed.

An efficient coupling between an intense laser pulse and a plasma takes place near the critical density, n_c , where the laser frequency equals to the local plasma frequency. In consequence, this interaction regime has been intensively investigated by theoreticians for two decades [1–9], and a great variety of nonlinear phenomena strongly depending on the coupling conditions has been unravelled: an efficient pulse absorption [1], magnetic self-channeling [3], plasma instabilities and nonlinear coherent structures [4–6], electron and ion acceleration [2]. Concerning the latter, recent experimental data have reported high-quality ion beams using very rare CO_2 lasers [10, 11], and emphasized as well the crucial role of the energy transfer process from the pulse to the plasma for such achievements with high potential.

However, this process stays largely unexplored, let alone controlled. The main reason is that, with common visible or near-infrared (IR) lasers, very few experimental studies could be reported so far in this regime, owing essentially to the technical difficulties of creation of controllable and reproducible plasmas with near-critical densities at these laser wavelengths. The known methods in this case consist in either exploding a thin solid foil in vacuum [12, 13] or in using foam targets [14, 15]. The exploding foil technique requires energetic laser pulses, that are difficult to control, and hydrodynamic simulations to predict the plasma density profile. A foam is a micro-structured material that is difficult to prepare, handle and simulate. Both methods suffer from a low repetition rate and shot-to-shot irreproducibility due to the fluctuations of laser and target parameters.

Here, we report for the first time on the collapse of an intense laser pulse in a near-critical plasma for IR-lasers and associated observed phenomena, unveiling new aspects of the energy transfer from the pulse to the plasma. We present in details an overall situation that recently attracted the attention of authors of theoretical studies

[2, 8, 9], but was never described in experiments to our knowledge. For that, we used a compact 10 Hz near-IR laser and a reproducible high density helium gas jet target [16]. With that latter device, one can create a plasma with the electron density up to $(3-5) \times 10^{21} \text{ cm}^{-3}$ within a spatial size of less than 1 mm. The pump-probe diagnostics reveal a laser channelling and energy deposition in a small plasma volume much before the critical density. A subsequent hot and dense electron cloud forms an ultrafast ionizing shock front and expands far from the laser axis ($\sim 150 \mu\text{m}$) at a velocity of about one-third of the light velocity ($c/3$). This was never measured before in gas jets, and thus raises the question of what does actually sustain such an ultrafast blob. Interestingly in our conditions, ion acceleration is observed at each shot only along the direction transverse to the laser axis, and occurs in fact before the pulse collapse region. We suggest in the following some practical elements that could lead to an ion beam generation along the laser axis after the laser has collapsed.

Our observations differ from the experiment with a foil-gas-foil package [17] where the laser energy was deposited in the foil with no given experimental detail on that process, and the ionizing shock in the gas caused by hot electrons had a velocity lower by an order of magnitude. In fact, the expansion velocity is in our case comparable to the plasma expansion rates measured in solid dielectric targets a decade ago [18, 19]. Here, in contrast to the solid targets, the ionizing shock front is formed on a *collisionless* timescale of less than 1 ps, so that its velocity indicates the energy in the collapse zone, and the transition from a collisionless to a collisional regime is smoothly covered.

The experiment was carried out at the Laboratoire d'Optique Appliquée, using an ultrashort Ti:Sapphire laser “Salle Jaune” with the pulse duration ~ 35 fs and the energy on target 810 mJ. The laser was focused on a

submillimetric supersonic helium jet to the focal spot of $20\text{ }\mu\text{m}$ full width at half maximum (FWHM). The normalized laser vector potential was $a_0 = 2.7$. The experimental setup was described in details [20] and enables a simultaneous detection of ion acceleration (along and transverse to the laser axis), the electron plasma density and the azimuthal magnetic field with respect to the laser propagation axis. The plasma optical probing is achieved with a spatial resolution of the order of $1\text{ }\mu\text{m}$ and with a temporal resolution equal to the duration of the frequency-doubled probe beam ($\sim 40\text{ fs}$).

The gas jet density distribution is shown in Fig. 1. The peak density in the jet exponentially decreases along the vertical Z direction with the characteristic scale length of $\sim 170\text{ }\mu\text{m}$, as the nozzle produces an expanding flow with a Mach number 1.5. The radial density profile at the distance of $200\text{ }\mu\text{m}$ from the nozzle exit is fit by: $n_e = 0.95 n_c \exp[-(r/r_0)^{2.5}]$, where $r_0 = 263\text{ }\mu\text{m}$ is the jet radius. Though the peak density could be tuned up, we kept it at that value, so that the collapse and the plasma expansion could happen within the field of view of our diagnostics.

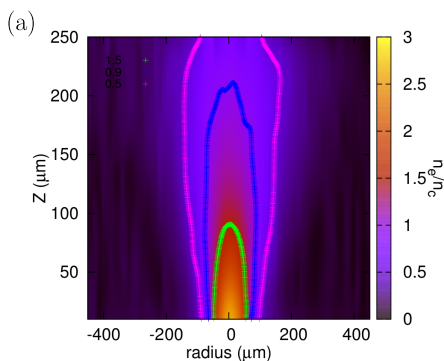


FIG. 1: Electron density n_e map (twice the atomic density interferometrically measured). Color contours are corresponding to $n_e = 0.5$ (pink), 0.9 (blue) and 1.5 (green) n_c .

The temporal evolution of the plasma is presented in Fig. 2 for the same plasma conditions. The laser propagates along the y -axis and it is linearly polarized along x -axis. All panels in Fig. 2 are in the y - z plane. On the left side of Fig. 2(a), 200 fs after the onset of the interaction, the plasma channel radius is much smaller than the laser beam width due to self-focusing [21]. The laser beam penetration terminates with a collapse [7, 8] well before the beam reaches the critical density. The on-axis bright spots, from plasma self-emission integrated with the CCD camera, are likely to indicate the longitudinal position where the laser pulse collapses. At this location, the laser breaks up into several filaments as can be seen later in panel (b), at 1.2 ps delay. Here, a striking circular plasma structure with sharp edges has grown asymmetrically about the laser, with its center located near the

middle of the jet. This structure appears opaque to the probe beam, probably due to the strong refraction and absorption of that beam. Formation of such a structure results from the ionization of the dense gas by the cloud of hot electrons [17–19], efficiently heated in the small volume where the pulse has collapsed, and collisionlessly expanding until about 1 ps.

In panel (c), in the collisional regime at 3.3 ps delay, the walls of the channel (on the left side of the figure) have started to expand and thicken. The blob appears now elliptical and elongated along the laser propagation direction, with a forward burgeoning bubble developing ahead of the structure in the falling part of the jet, and separated from the main structure by a vertical bright edge. This secondary structure might be analogous to the dense plasma blocks (“light bullets”) observed in the collisional regime near the critical density and moving along a decreasing density gradient [22]. We did not investigate further that unclear point which will be clarified in a future study.

We believe that the collapse abruptly terminates the continuous laser-to-plasma energy conversion process acting efficiently when the pulse propagates in the long and dense plasma [2, 9, 23]. This well explains why the pulse does not reach the critical density and why an observable dense cloud is initiated from a point-like region. As the peak density is slightly decreased, the collapse and the opaque cloud are seen to move towards the center of the jet. When the peak density is reduced down to about $n_e \sim 0.2 n_c$, the pulse manages to channel through the plasma and similar non-linear coherent structures as in Ref. 20 could be observed, until about $n_e \leq 0.01 n_c$, where the images were blank at each shot. An elaboration of such a complex transition when decreasing the density is beyond the scope of the present report, but our data emphasize the determining role of pulse propagation conditions in the excitation of wake instabilities and high-density current generation in near-critical plasmas [9].

In order to confront quantitatively our observations to simulations, we precisely measured the expansion rate by choosing an axial coordinate where filaments do not significantly perturb the structure outer edges (see Fig. 3(a)). The time dependence of the opaque zone size along the yellow line is presented in panel (b). Each cut-off (see inset) maps out the transverse plasma density gradients. Each column in the map represents an average profile obtained from at least two shots in the same conditions.

The structure expands asymmetrically (inset in panel (a) and contours in panel (b)), the expansion being faster towards the nozzle (negative coordinates and increasing densities). The opaque structure is clearly visible from about $t_0 + 400\text{ fs}$ and we measured, over a timespan of 1 ps in the collisionless regime, average radial velocities in both downward and upward directions of $c/2$ and $c/3$,

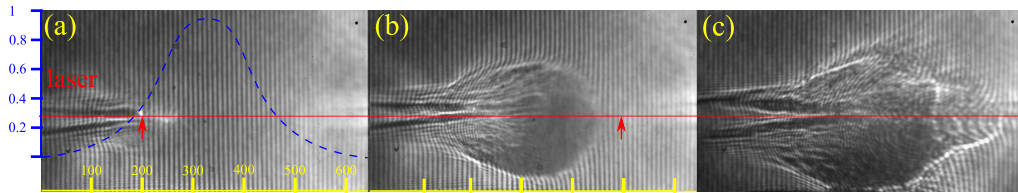


FIG. 2: Electron density interferograms for the peak density $n_e \approx 0.95n_c$ at the probe delays at: (a) $t_0 + 0.2$ ps, (b) $t_0 + 1.2$ ps and (c) $t_0 + 3.3$ ps, where t_0 corresponds to our reference time (onset of the interaction). The blue dotted line in (a) maps out the electron density profile at the laser axis height (blue scale in unit of n_c). The yellow scale is in microns. The small red arrows indicate the position of the laser pulse assuming the laser group velocity equal to c . From $\sim t_0 + 0.4$ ps, the spherical structure is opaque to the probe beam.

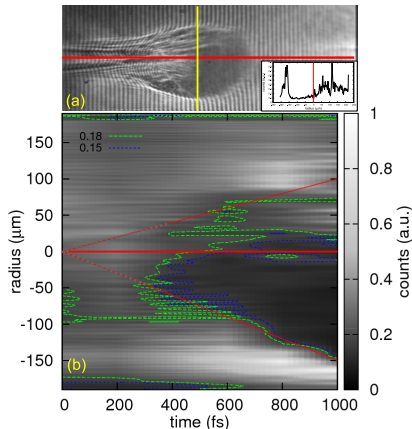


FIG. 3: Asymmetric ultrafast radial expansion: (a) interferogram at $t_0 + 1$ ps. Inset: cutoff along the yellow line. (b) Cutoffs along the yellow line in panel (a) versus time. Horizontal solid red line shows the laser axis. Isolines at the levels 0.15 (dashed blue) and 0.18 (dashed green) show the opaque structure formation. Oblique solid red lines indicate the expansion velocity $c/3$ upstream and $c/2$ downstream (red dotted lines to guide the reader).

respectively (see oblique red lines in panel (b)). These radial expansion velocities of electron fronts are higher by an order of magnitude than other reported measurements at lower plasma densities [24]. The measurements in the upper part panel (b) are affected by a noise due to the presence of several filaments, but the front stays trackable. The similar analysis leads to an expansion velocity of $\sim c/2$ in the laser propagation direction. However, this fast cloud expansion slows down after the first picosecond and further plasma evolution proceeds much slower, which indicates that the collisional regime has been reached.

The formation of a channel without soliton/vortex before the collapse is corroborated by the experimental detection of energetic ions in the direction *transverse* to the laser beam axis, as an anticorrelation is expected [20], and numerical simulations show also that this acceleration takes place in the channel formed prior to the collapse. For each shot, we consistently measured He^+ ions

with energies up to 250 keV. No ion could be detected in the longitudinal direction at any plasma density we tested within the range $n_e = 0.01 - 5 n_c$. This is certainly because of low current density from hot electron divergence at the falling part of the jet, where acceleration is supposed to take place [2, 25, 26]. With the same gas profile as in Fig. 1 and about three times more energy in the short pulse (~ 100 TW laser), an ion beam in the *longitudinal* direction should be detected reproducibly, as the laser pulse will collapse later in the jet, implying higher hot electron density current at the back and a strong longitudinal electric field [2, 9]. With our pulse energy, a shorter plasma could also be considered to obtain high hot electron density current at the falling part of the jet. However, this would have required to entail a similar strong self-focusing and collapse a much higher backing pressure (> 400 bar), which we could not hold with our gas jet system.

To challenge our measurements and unveil the mechanisms in the collapse region, the experiment was simulated with the particle-in-cell code PICLS [27]. This is fully electromagnetic $2D \times 3V$ kinetic code that accounts for the electron-electron and electron-ion collisions and the atom field ionization. The laser and plasma parameters correspond closely to the experimental ones. A laser pulse of the dimensionless amplitude $a_0 = 2.2$, of wavelength $0.8 \mu\text{m}$, of duration 29 fs FWHM and of transversal size $24 \mu\text{m}$ FWHM was injected horizontally in a helium gas, with a linear density profile with a scale length of $200 \mu\text{m}$ along the vertical direction, and a parabolic density profile with the same scale length along the laser propagation axis. The maximum electron density at the top of the plasma profile was $0.91 n_c$ assuming the complete ionization.

The laser pulse undergoes strong self-focusing that ends up with a beam collapse in the plasma ramp at density $n_e \sim 0.2 n_c$, close to the experimental value $\sim 0.27 n_c$. As mentioned before, the numerical simulations show ion acceleration in the transverse direction from the channel before the collapse zone. The ion energies are in the range of a few hundred keV in good agreement with the observations. In the collapse region, a significant part of the laser pulse energy of a few tenths

of joule is released in a volume with the characteristic size of less than $20\ \mu\text{m}$. The electrons acquire in there energies up to a few MeV and stream away with relativistic velocities. An extremely high electric current associated with these electrons leads to strong magnetic fields forming a dipole structure similar to the one described in Ref. 9 (see Figure 4).

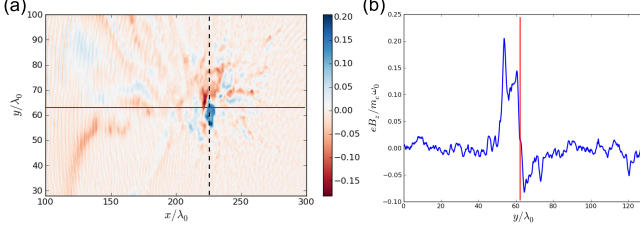


FIG. 4: (a) Map of the normalized magnetic field along z and (b) lineout along the dashed line at $t = t_0 + 1.27$ ps. The laser axis is in red.

The magnetic field intensity is of the order of 10 MG, and the magnetic field energy in the collapse zone is comparable to the hot electron kinetic energy. Because of total opacity of the cloud in experiments, we did not manage to assess the magnetic field in the collapse region with our optical Faraday-effect polarimeter [20], but third-harmonic probe beam or proton radiography are likely to be relevant alternatives.

The hot electron cloud creates a strong electrostatic field at its edge that ionizes the ambient gas far from the laser axis and creates a return current of plasma electrons. This process of plasma ionization by a beam of energetic electrons has been theoretically described in an 1D geometry [28, 29]. The velocity of the corresponding ionization front $\sim 0.7c$ observed in simulations is slower than the fast electron velocity as an accumulation of the electron density is necessary to generate a sufficiently strong electric field, comparable to the atomic field. This front velocity is higher than that of the experiments ($\sim 0.5c$), since our 2D simulation model overestimates the ionization front velocity because of slower electron cloud divergence as in the real 3D experiment.

Fast electron propagation and plasma ionization obtained in the numerical simulation 900 fs after the laser pulse collapse are shown in Fig. 5. The collapse point is located at $x = 226\lambda_0$ and $y = 63\lambda_0$. This point is the origin of the electron cloud propagating radially. Panel a) shows three groups of electrons with the different energies. The width of the electron cloud is about $80\ \mu\text{m}$, which is much wider than the laser pulse in vacuum. This width depends on the magnetic dipole lifetime created in the collapse zone and sustaining the electron heating. The outer boundary of the electron cloud outlines the plasma edge, meaning that the electron cloud is responsible for the ionization of the gas. This can be seen in panel b) showing the electron plasma density and the

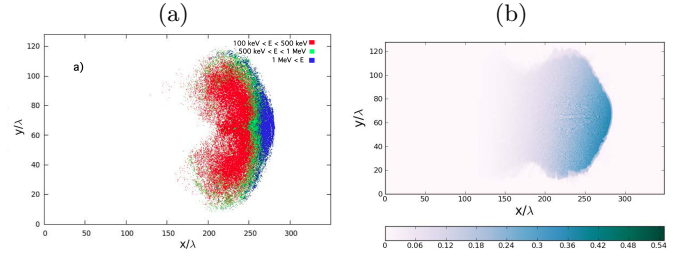


FIG. 5: (a) Distribution of energetic electrons at $t = t_0 + 0.9$ ps and (b) electron plasma density. The plasma density in the collapse point is $0.2n_c$. The ionization of the gas unveils a vertical density gradient in panel (b).

electric field averaged over the laser period. The electric field amplitude at the cloud edge $\sim 0.1 m_e c \omega_0 / e$ is of the order of the atomic field $eE_{at} / m_e c \omega_0 \simeq 0.13$. That is sufficient for double ionization of helium within a characteristic time of a few femtoseconds. As time goes on, the fast electrons that are propagating through the gas and ionizing it, lose their energy in the self-consistent electric field. The stopping power is of few tens of $\text{keV}/\mu\text{m}$, therefore, in one picosecond time scale the fast electrons are reducing their energy to a few keV thus transforming a free streaming into a collisional diffusion.

In conclusion, our experiment demonstrates intense laser pulse channelling in a low density gas or plasma, terminated with a violent collapse as soon as the gas density exceeds a few tens of percent of the electron critical density. The channel formation without wake instabilities and its expansion leads to the transverse acceleration of energetic ions. The very abrupt absorption of the laser pulse energy in the collapse zone leads to the acceleration of relativistic electrons accompanied with the creation of a long-lasting magnetic dipole structure that further accelerates electrons. Consequently, the current of fast electrons manages to sustain an ionization front propagating collisionlessly over a large region in the gas, at a velocity comparable but less than the light velocity. Our experimental results shed new light on fundamental aspects of the interaction in near-critical regime, paving the way for instance towards controllable giant magnetic dipole generated in a decreasing plasma gradient [2], of great interest for efficient ion acceleration with a gas jet.

The authors acknowledge the support of OSEO project n.I0901001W-SAPHIR, the support of the European Research Council through the PARIS ERC project (contract 226424), and the National research grant ANR-08-NT08-1-38025-1. This work was partially supported by EURATOM within the "Keep-in-Touch" activities and the Aquitaine Region Council. Also, it was granted access to the HPC resources of CINES under allocations 2011-056129 and 2012-056129 made by GENCI (Grand Equipement National de Calcul Intensif).

-
- [1] S. C. Wilks *et al.*, Phys. Rev. Lett. **69**, 1383 (1992).
 - [2] T. Nakamura *et al.*, Phys. Rev. Lett. **105**, 135002 (2010).
 - [3] A. Pukhov and J. Meyer-ter-Vehn, Phys. Rev. Lett. **76**, 3975 (1996).
 - [4] S. V. Bulanov *et al.*, Phys. Rev. Lett. **76**, 3562 (1996).
 - [5] S. V. Bulanov *et al.*, Phys. Rev. Lett. **82**, 3440 (1999).
 - [6] T. Esirkepov *et al.*, Phys. Rev. Lett. **89**, 275002 (2002).
 - [7] W. B. Mori *et al.*, Phys. Rev. Lett. **60**, 1298 (1988).
 - [8] G. Li *et al.*, Phys. Rev. Lett. **100**, 125002 (2008).
 - [9] T. Nakamura and K. Mima, Phys. Rev. Lett. **100**, 205006 (2008).
 - [10] C. A. J. Palmer *et al.*, Phys. Rev. Lett. **106**, 014801 (2011)
 - [11] D. Haberberger *et al.*, Nat. Phys. **8**, 95-99 (2011)
 - [12] M. Borghesi *et al.*, Phys. Rev. Lett. **78**, 879 (1997).
 - [13] A. Yogo *et al.*, Phys. Rev. E **77**, 016401 (2008).
 - [14] L. Willingale *et al.*, Phys. Rev. Lett. **102**, 125002 (2009).
 - [15] S. Okihara *et al.*, Phys. Rev. E **69**, 026401 (2004).
 - [16] F. Sylla *et al.*, Rev. Sci. Instrum. **83**, 033507 (2012)
 - [17] D. Batani *et al.*, Phys. Rev. Lett. **94**, 055004 (2005).
 - [18] M. Borghesi *et al.*, Phys. Rev. Lett. **83**, 4309 (1999).
 - [19] L. Gremillet *et al.*, Phys. Rev. Lett. **83**, 5015 (1999).
 - [20] F. Sylla *et al.*, Phys. Rev. Lett. **108**, 115003 (2012).
 - [21] G. Sun *et al.*, Phys. Fluids, **30**, 526-532 (1987).
 - [22] N. I. Vogel *et al.*, Phys. Rev. Lett. **86**, 232 (2001).
 - [23] F. Fiuza *et al.*, Plasma Science, IEEE **39**, 2618 (2011).
 - [24] P. M. Nilson *et al.*, Phys. Rev. Lett. **103**, 255001 (2009).
 - [25] L. Willingale *et al.*, Phys. Rev. Lett. **96**, 245002 (2006)
 - [26] S. V. Bulanov *et al.*, Phys. Rev. Lett. **98**, 049503 (2007).
 - [27] Y. Sentoku and A. Kemp, J. Comput. Phys. **227**, 6846 (2008).
 - [28] S. I. Krasheninnikov *et al.*, Phys. Plasmas **12**, 073105 (2005).
 - [29] A. Debayle and V. T. Tikhonchuk, Phys. Plasmas **14**, 073104 (2008).